Indian J. Phys. **72A** (6), 601–619 (1998)

IJP A
— an international journal

Quark gluon plasma—current status of properties and signals

C P Singh*

Department of Physics, Banaras Hindu University,
Varanasi-221 005, India

Abstract : The current status of properties and signals of quark gluon plasma (QGP) is reviewed. We find that the simple equations of state (EOS) used for the description of QGP as well as hadron gas (HG) shold be properly modified to account for the interactions present. We briefly review the promising signatures existng in the literature. We find that the recent J/Ψ suppression observed by NA50 experiments gives a clear hint for the deconfinement phase transition. We discuss how the variation of $\phi/(\rho + \omega)$ with energy density can yield an unambiguous signal for QGP formation. Finally we discuss the recent work connected with the baryon-density inhomogeneity created in the early universe due to a quark-hadron phase transition.

Keywords : Quark gluon plasma, heavy ion collisions, equation of state, hadron gas, early universe

PACS Nos. : 25.75.–q, 21.65.+f, 12.39.Fe

1. Introduction

QCD predicts the existence of a phase transition from an ordinary hadronic matter to a plasma of quarks and gluons (QGP) whenever the energy density ε exceeds its value existing inside a proton ($\varepsilon_p \simeq 0.5$ GeV/fm^3). A large energy density can be achieved in two ways : either by compression which means putting more and more particles in a given volume, or by heating the vacuum which means increasing the particle kinetic energies. In the new phase hadrons dissolve into weakly interacting quarks and gluons and an ideal colour-conducting plasma of quarks and gluons is formed. In a QGP medium, the long range colour force is Debye screened due to collective effects in the same way as noticed in the case of an electromagnetic plasma. In QCD, the potential consists of two parts : one coulombic part and the other is a linearly rising confinement potential. The long range behaviour of this potential is screened in a dense medium as $\sigma r \rightarrow \sigma r_D (1 - e^{-r/r_D})$. Thus at very high density when $r \leq r_D$, colour screening will dissolve a hadron into its coloured

e-mail cpsingh @ banaras.ernet.in

quark constituents so that a colour-conducting phase appears from a colour-insulator phase through a deconfining phase transition.

The discovery and proper understanding of QGP is of paramount significance for QCD since it foretells the long-range behaviour where the theory is still poorly understood. The two different phases correspond to different states of vacuum in QCD : the perturbative vacuum in which quarks and gluons propagate almost freely and the physical, non-perturbative vacuum which is relevant for the low-energy hadrons. Phase transition in QCD at high temperature is useful in the cosmological studies, *e.g.* possible formation of a baryon number inhomogeneity which persists to the epoch $T \simeq 100$ MeV could affect primordial nucleosynthesis yields of light elements. Such inhomogeneity can also result in the formation of a stable or metastable strange quark nugget and it can also explain the dark matter. It has also been suggested that primordial black holes and primordial magnetic fields can originate in a first order QCD phase transition. The QGP phase of matter can also provide a key information about the inner core of a neutron star having a very large nuclear density.

Ultra-relativistic heavy-ion collisions provide us the opportunity to search for the QGP formation in the laboratory. A large number of particles produced in a finite volume of the collision give rise to a large value of energy density. Such a large energy density can be achieved in two ways (which is shown schematically in Figure 1a) : either by heating the nuclear matter so that the kinetic energy of the particles becomes higher or by compressing the matter so that the baryon density becomes extremely large. The evolution of produced matter is governed by relativistic hydrodynamics which is shown in Figure 1b. In both the cases the hadrons come closer to each other and the distance between the quarks decreases resulting in a very weak force between them. The phase diagram of hadron gas and QGP has been shown in Figure 2. One expects that the hadrons exist in the low density, low temperature region while the high density, high temperature region is populated by quarks and gluons. The precise determination of the critical line is done by using the Maxwell's construction of the first-order equilibrium phase transition.

The simplest QCD motivated model which indicates the formation of QGP is the bag model of hadrons. In the bag model, a hadron consists of a set of quarks moving freely inside a bag of finite dimension and quarks acquire infinite mass outside the bag. Free quarks and gluons can only propagate where the complex structure of QCD vacuum has been destroyed. The value of the vacuum pressure B represents the energy required as a result of such kind of vacuum re-alignment. In other words, the phenomenological quantity summarises the interaction effects which are responsible for a change in the vacuum structure between the low temperature and the high temperature phases. Minimising the energy of a spherical bag, one gets the equilibrium energy density inside a proton $\varepsilon_0 = 4\,B$ which is also the latent heat density required for a deconfining phase transition. If the pressure of the quark matter inside the bag is increased, there will be a point when the outward pressure arising due to the kinetic energy of the quarks becomes larger than the inward vacuum pressure B. In such situations, the bag cannot confine the quarks and it will

result into a new deconfined phase. The pressure of the quark matter increases when the temperature of the matter is large enough and/or the baryon density is quite large.

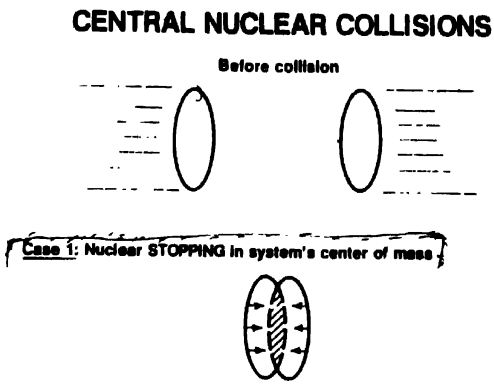

Figure 1(a). Schematic diagram of ultra-relativistic nucleus-nucleus collision.

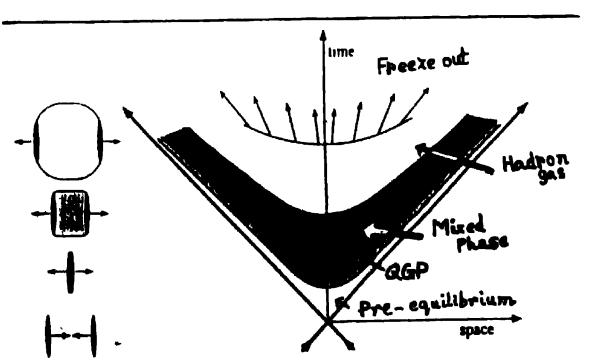

Figure 1(b). Space time evolution diagram in a nucleus-nucleus collision.

The QCD Lagrangian is written as

$$\mathcal{L} = \bar{\psi}_j \left(i\gamma_\mu D^\mu_{jk} - m_{jk} \right) \psi_k - \frac{1}{4} F^{\mu\nu}_a F^a_{\mu\nu} \tag{1}$$

where the indices a, j, k are the colour-indices ($a = 1 \cdots 8$; $j, k = 1 \cdots 3$) and the covariant derivative is

$$D^\mu_{jk} = \delta_{jk} \partial^\mu + ig(T_a)_{jk} G^\mu_a \tag{2}$$

Similarly the gluon field tensor is

$$F^{\mu\nu}_a = \partial^\mu G^\nu_a - \partial^\nu G^\mu_a - g_s f_{abc} G^\mu_b G^\nu_c \tag{3}$$

Here G^μ_a are the gluon fields, T_a are the SU(3) colour generators, g_s is the strong coupling, m_{jk} is the quark mass matrix and f_{abc} are the structure constants of $SU(3)_C$. An important symmetry of $\mathcal{L}_{QCD}$ in eq. (1) is the chiral symmetry. For massless fermions $\mathcal{L}_{QCD}$ is invariant under global flavour rotations U_R and U_L for right and left handed spinors. For N_f flavours,

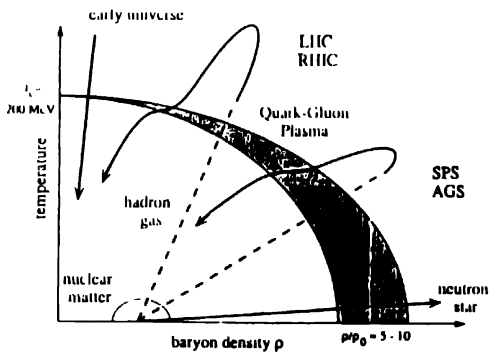

Figure 2. Phase diagram of the strongly interacting matter showing the hadronic phase at low temperature and baryon density, the transition region (mixed phase), and the QGP phase

the matrices are $N_f \times N_f$ and they form a group $U(N_f) \times U(N_f)$ which has a proper chiral subgroup $SU(N_f) \times SU(N_f)$. For $N_f = 2$, the group is $SU(2) \times SU(2)$ and two Noether currents for a combined flavour and γ_5 transformations are $V^a_\mu = \bar{\psi}\gamma_\mu(\tau_a/2)\psi$ and $A^a_\mu = \bar{\psi}\gamma_\mu\gamma_5(\tau_a/2)\psi$, where τ_a's are the Pauli isospin matrices. The vector current is conserved corresponding to isospin-invariance. However, partially conserved axial current satisfies PCAC relation $\partial^\mu A^a_\mu = C_\pi \phi_\pi$ where ϕ_π is the pion field. It means that the vacuum is not invariant under isoaxial rotations and hence the vacuum expectation value of operators $\langle \bar{\psi}\psi \rangle \neq 0$.

2. Lattice calculations

Phase transitions can be examined through the behaviour of an order parameter. A discontinuous change in the order parameter at the critical point characterizes a first order

phase transition. For a second order phase transition, the order parameter changes continuously. In lattice gauge theory, one evaluates [5] the partition function.

$$Z(T, V) = \int d\psi d\bar{\psi} dG_\mu \exp \int_0^{1/T} d\tau \int_V d^3 x \mathfrak{L} \tag{4}$$

on a discretized space-time as a lattice of points with a_σ and a_τ as lattice spacings in space and time directions, respectively so that $V = (N_\sigma a_\sigma)^3$ and $T = (N_\tau a_\tau)^{-1}$. Thus infrared and ultraviolet divergences are properly handled in the discretized lattice formulation with ψ and $\bar{\psi}$ as site variables. The link variable between two sites $U_\mu(x) = \exp\left[ig_s a \sum_1^8 \lambda^l G_\mu^l(x)\right]$ represents rotations in colour space. Finally, we find that the structure becomes equivalent to spin system and can be evaluated in an analogous way.

In order to determine the order of deconfinement phase transition in lattice calculations, one evaluates the order parameter as the expectation value of Wilson loop variable $< L > = \exp[-F/T]$ where F is the energy of a quark. Since $F \to \infty$ in the confinement regime, we get $< L > = 0$ but in the deconfined region, $< L >$ = constant (> 0). Similarly order parameter for chiral phase transition is $\langle \bar{\psi}\psi \rangle$ and is a constant greater than zero for the constituent quarks but is zero for current quarks. In Figures 3(a,b), we show the

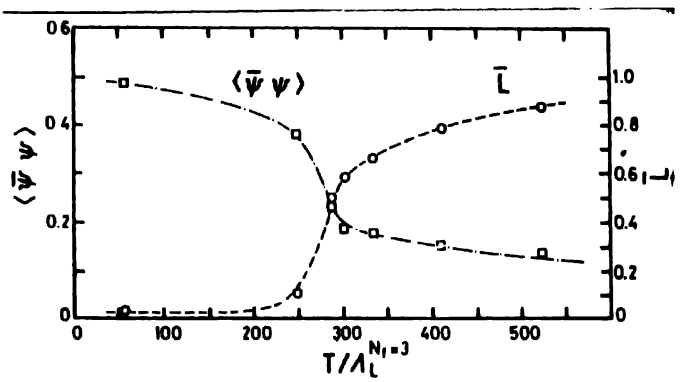

Figure 3(a). Deconfinement measure $<L>$ and chiral symmetry measure $< \bar{\psi}\psi >$, on a $8^3 \times 4$ lattice.

results of lattice gauge calculations and these results suggest that both these phase transitions occur almost at the same temperature. They are also first order phase transition because they involve a sudden change in energy density ε. Similarly, a quantity $(\varepsilon - 3P)/T^4$ which yields a measure for an ideal gas behaviour is not zero even at $T \simeq 2T_c$ and thus it involves considerable plasma interactions. When there are quarks in the theory, there is a

big difference in physics for $N_f = 0, 2, 3$ flavours respectively. Critical temperature depends on the number of flavours ($T_c \propto N_f^{-1/2}$). Similarly for $N_f = 2$ massless quarks, we get a continuous transition. For $N_f \geq 3$ massless quarks, the phase transition is of first order but for $N_f \simeq 3$ with two massless u, d quarks and $m_s > 0$, we again get a continuous transition. However, lattice simulations for $n_B \neq 0$ involve some technical troubles and the calculations are not unambiguous ones.

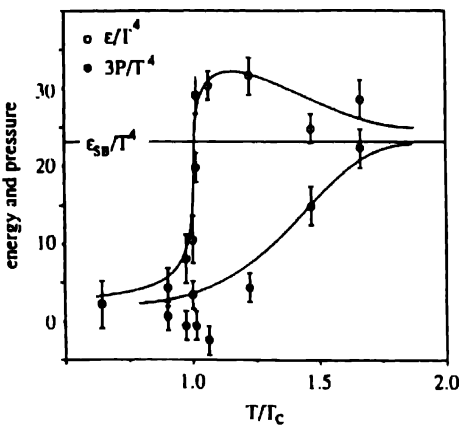

Figure 3(b). The energy density ε and the pressure $3P$, normalised to the ideal Boltzmann gas limit, according to lattice calculations

One can construct first order phase transition by using Gibbs criteria for equilibrium phase transition $P_{HG} = P_{QGP}$, $T_{HG} = T_{QGP}$, $\mu_{HG} = \mu_{QGP}$ at the critical point. In other words, one uses the condition

$$P_{HG}(T_c, \mu_c) = P_{QGP}(T_c, \mu_c). \tag{5}$$

However, one can obtain pressure in hadron gas (HG) or in QGP phase provided one has the proper knowledge of realistic equations of state (EOS) in both phases separately. If one simply write $P_H = P_Q - B$ for the case $\mu = 0$ in eq. (5) where B summarizes the interaction effect in QGP phase, one gets $T_c \simeq 0.72\, B^{1/4}$ or $T_c \simeq 140$ MeV for $B^{1/4} = 200$ MeV.

3. EOS for QGP

Recently there were some suggestions for modifying the EOS for QGP by giving a μ and T-dependence to the bag constant B. Let the QGP hadronize at fixed T and μ to a hadron gas (HG). If we calculate entropy per baryon (S/B) ratio, we find that

$$(S/B)_{QGP} > (S/B)_{HG} \tag{6}$$

This, however, violates the second thermodynamical principle. In order to cure this problem, either one should change T and μ during mixed phase which is often referred as subsequent dilution and reheating, or one can fix T and μ during phase boundary and

assume isentropic equilibrium phase transition so that $(S/B)_{QGP} = (S/B)_{HG}$. The price one has to pay is to assign a T and μ dependence to the bag constant. Thus

$$\frac{s_{QGP} - S^{C}_{QGP}}{n_{QGP} - n^{C}_{QGP}} = \frac{S_{HG}}{n_{HG}} \tag{7}$$

where the correction factors $S^{C}_{QGP} = \dfrac{\partial B(\mu, T)}{\partial T}$ and $n^{C}_{QGP} = \dfrac{\partial B(\mu, T)}{\partial \mu}$.

partition function for QGP with massless u, d quarks and gluons :

$$\frac{T \ln Z_{QGP}}{V} = \frac{T \ln Z_{Q}^{Ideal}}{V} + \frac{T \ln Z_{Q}^{Int}}{V} \tag{8}$$

where
$$\frac{T}{V} \ln Z_{Q}^{Ideal} = \frac{37}{90}\pi^2 T^4 + \frac{\mu^2 T^2}{9} + \frac{\mu^4}{162\pi^2} - B(\mu, T) \tag{9}$$

$$\frac{T}{V} \ln Z_{Q}^{Int} = -\alpha_s(\mu, T)\left[\frac{11}{9}\pi T^4 + \frac{2}{9\pi}\mu^2 T^2 + \frac{\mu^4}{81\pi^3}\right] \tag{10}$$

and
$$\alpha_s(\mu, T) = \frac{12\pi}{29}\left[\ln\left(\frac{0.8(\mu^2/9) + 15.622\,T^2}{\Lambda^2}\right)\right]^{-1} \tag{11}$$

For $T \to$ large and $\mu \to 0$ case, we get expression for $B(\mu, T)$ as

$$B(\mu, T) = B_0 + \frac{1}{9}\mu^2 T^2 + \frac{\mu^4}{162\pi^2} - \frac{148}{3\pi^2} m^2 T^2 K_2(m, T) \times [\cosh(\mu/T) - 1] - \alpha_s(\mu, T)\left[\frac{11}{9}\pi T^4 + \frac{2}{9\pi}\mu^2 T^2 + \frac{\mu^4}{81\pi^3}\right] \tag{12}$$

Similarly in the large density limit (*i.e.* $\mu \to$ large, $T \to 0$), we get

$$B(\mu, T) = B_0 + \frac{37}{90}\pi T^4 + \frac{1}{9}\mu^2 T^2 - \frac{1}{81}\frac{\mu^4 T^2}{\theta^2} - \frac{T^4\pi^2}{2430}\left(\frac{\mu}{\theta}\right)^3\left[7\frac{\mu}{\theta} - \frac{59}{2}\frac{m^2\mu}{\theta^3} + 3\right] - \alpha_s(\mu, T)\left[\frac{11}{9}\pi T^4 + \frac{2}{9\pi}\mu^2 T^2 + \frac{\mu^4}{81\pi^3}\right] \frac{\pi T^4}{324}\left(\frac{\mu}{\theta}\right)^4\left[\alpha_s\left(1 - \frac{\mu^2}{\theta^2}\right) + \mu\frac{\partial\alpha}{\partial\mu}s\left(\frac{9}{2} - \frac{\mu^2}{\theta^2}\right.\right. \tag{13}$$

where $\theta = (\mu^2 - m^2)^{1/2}$. We have shown the variations of $B(\mu, T)$ with μ and T in Figures (4–5) using eqs. (13) and (12), respectively. We find that $B(\mu, T)$ decreases and

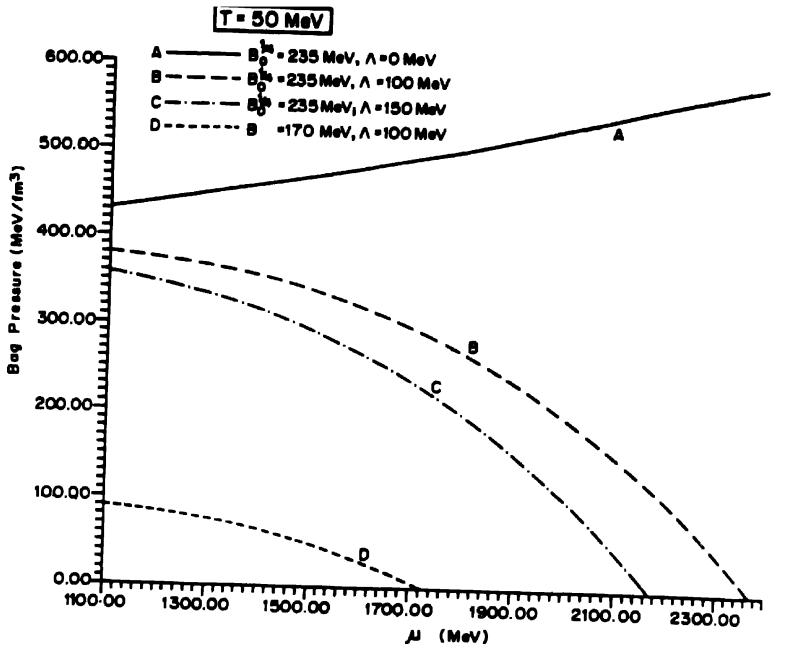

Figure 4. Variation of bag pressure $B(\mu, T)$ from eq (13) with baryon chemical potential (μ) at a temperature T = 50 MeV. Curve A represents the free QGP EOS with $B_0^{1/4}$ = 235 MeV. Curve B represents the interacting QGP EOS with QCD scale parameter Λ = 100 MeV and $B_0^{1/4}$ = 235 MeV and curve C for Λ = 150 MeV and $B_0^{1/4}$ = 235 MeV. In curve D we have used $B_0^{1/4}$ = 170 MeV and Λ = 100 MeV.

goes to zero also. Similar behaviour has also been obtained in other models as well. From eq. (12), it is obvious that at $\mu = 0$ we get

$$B(\mu = 0, T) = B_0 \left[1 - \left(\frac{T}{T_0}\right)^4\right] \tag{14}$$

where $T_0^4 = \dfrac{9B_0}{11\pi\alpha_s(0, T)}$. Similarly at $T = 0$, we get from eq. (13):

$$B(\mu, T = 0) = B_0 \left[1 - \left(\frac{\mu}{\mu_0}\right)^4\right] \tag{15}$$

where $\mu_0^4 = \dfrac{81\pi^2}{\alpha_s(\mu, 0)} B_0$. These kinds of equations have also been obtained in other models like QCD sum rules *etc.*

In Figure 6 we have shown the critical phase boundary obtained when $B(\mu_c, T_c) = 0$. This phase boundary signifies the transition from hadronic matter to a plasma of completely free quarks and gluons. For comparison, we have also shown the phase boundary obtained

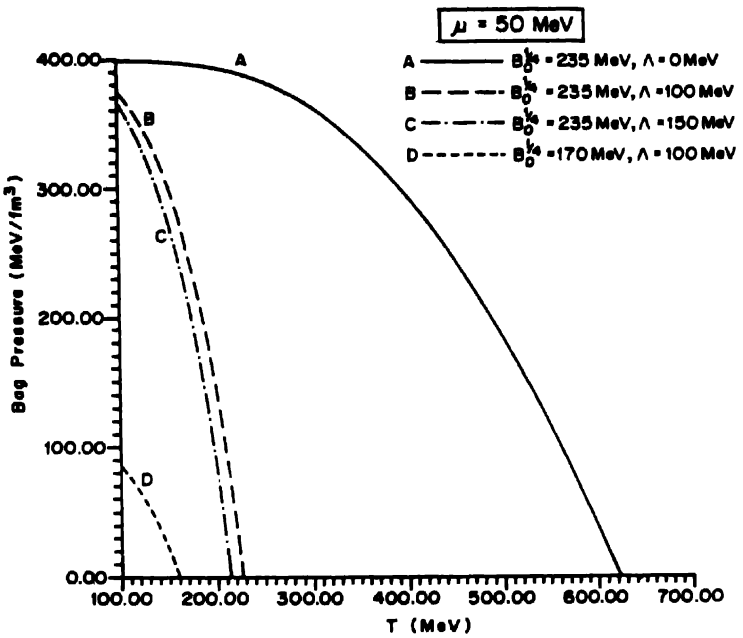

Figure 5. Variation of bag pressure as obtained from eq. (12) with temperature (T) at constant baryon chemical potential μ = 50 MeV. The notations are the same as in given in Figure 4.

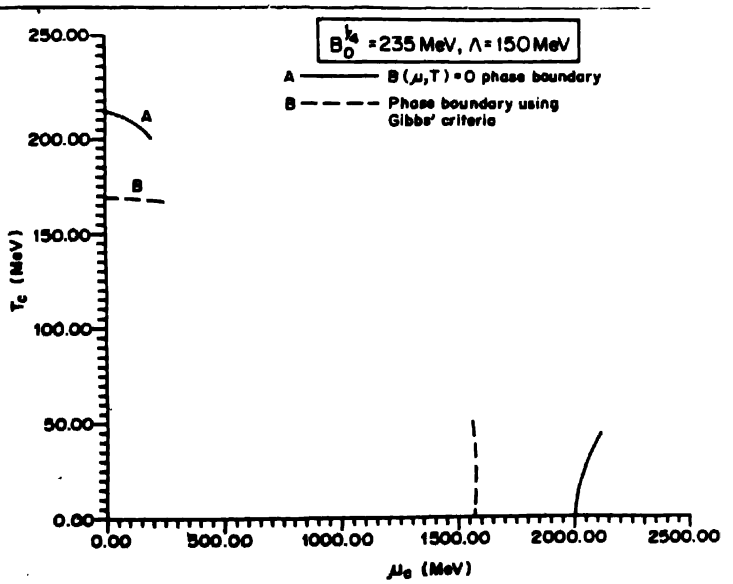

Figure 6. Critical curve obtained from the equation $B(\mu_c, T_c) = 0$ is shown by a solid line (curve A) in the two extreme regions of large T_c, low μ_c and large μ_c, low T_c, respectively. The corresponding critical curve obtained for the Gibbs condition of the pressure equality is shown by a dashed line (curve B).

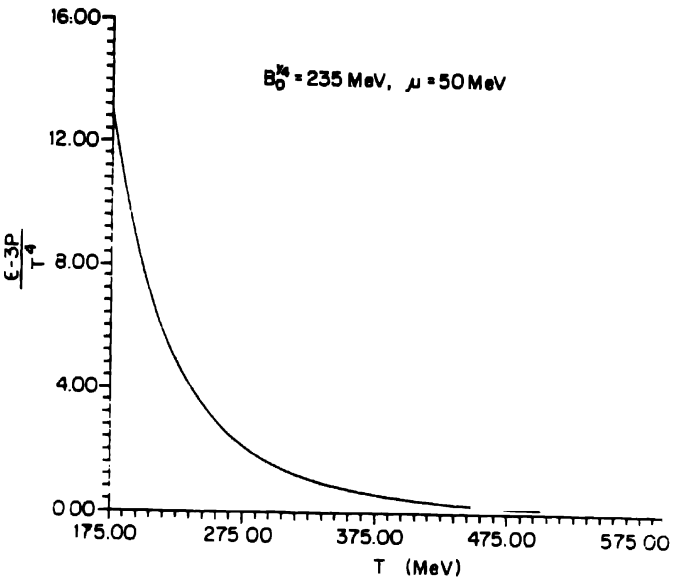

Figure 7. Variation of $(\varepsilon-3P)/T^4$ with temperature (T) for $\mu = 50$ MeV and $B_0^{1/4} = 235$ MeV

using Gibbs criteria in isentropic phase transition. In Figure 7, we have demonstrated the variation of $(\varepsilon - 3P)/T^4$ with temperature T and we find the curve agrees with that obtained in lattice gauge calculations.

4. EOS for hadron gas

We can make attempt to modify the equation of state (EOS) for a hot and dense hadron gas. At a large T and μ, a large number of resonances are also present in the hadron gas giving rise to a large interaction. Attractive interactions can be accounted well by considering a large number of resonances in the HG. The main problem is how to account for the repulsive interactions in the proper EOS for HG. It has earlier been demonstrated that we must consider repulsive interactions in the HG at large μ and T, otherwise we do not get a unique phase transition point. Repulsions have been considered either by considering mean field type approaches [14] or by using excluded volume approach [9–13] in which we give a finite hard-core volume to each baryon. In the mean field approach, the repulsive interaction results from $\omega(783\,\text{MeV})$ meson exchange potential $V(r) = -\frac{g_\omega}{r}\exp(-m_\omega r)$ between two nucleons and hence it generates a potential energy $W(n_B) = \frac{4\pi g_\omega^2}{m_\omega} n_B$ in a hadron gas with a net baryon density n_B. In the case of early universe $n_B = 0$, so $W(n_B) = 0$ although HG contains a very large number of nucleons, anti-nucleons and pions. In such situations, excluded volume approach is more successful and we write the expression for free volume $V' = V - \Sigma_i N_i V_i$ where N_i is the total number of

baryons of i-th kind and V_i is the proper volume of one such baryon. Thus the excluded volume $\Sigma_i N_i V_i$ is subtracted from total volume. Thus Cleymans and Suhonen [10] got for the net baryon density $n_i = n_i^0/(1 + \Sigma_i n_i^0 V_i)$, where n_i^0 is the net baryon density of i-th pointlike baryon species. Kuono and Takagi suggested that the repulsion exists either between a pair of baryons or between a pair of antibaryons and thus we get :

$$n_B = \frac{n_B^0}{1 + \sum_i n_{B,i}^0 V_B} - \frac{n_{\bar{B}}^0}{1 + \sum_i n_{\bar{B},i}^0 V_B} \tag{16}$$

In the Hagedron model, we get excluded volume proportional to pointlike energy density so that

$$n_B = \frac{n_B^0}{1 + \varepsilon^0/4B}, \qquad \varepsilon = \frac{\varepsilon^0}{1 + \varepsilon^0/4B} \tag{17}$$

At large T, $\varepsilon^0/4B \gg 1$, so that $\varepsilon = 4B$. However, all these approaches lack thermodynamical consistency, Rischke *et al* [11] proposed the following modification to the grand partition function

$$Z^G(T, \beta, V - V_B N) = \sum_{N=0}^{\infty} e^{\mu N/T} Z^C(T, N, V - NV_B)\,\theta(V - NV_B) \tag{18}$$

and then define the pressure partition function as

$$\hat{Z} = \int dV e^{-\xi V} Z^G(T, \mu, V - V_B N) \tag{19}$$

If we put $\tilde{\mu} = \mu - TV_B\xi = \mu - V_B P^{\text{excl}}$, we shall get :

$$\hat{Z} = \int dx\, e^{-\xi x} Z^G(T, \tilde{\mu}, x) \tag{20}$$

so that we get a transcendental equation as

$$n^{\text{excl}}(T, \mu) = \frac{n_B^0(T, \tilde{\mu})}{1 + V_B n_B^0(T, \tilde{\mu})} \tag{21}$$

obviously these equations are difficult to solve.

Recently, we formulated one unique way to incorporate excluded volume correction in a thermodynamically consistent way by directly doing the volume integral :

$$\ln Z_i = \frac{g_i \lambda_i}{6\pi T^2} \int_{V_i}^{V - \sum_j V_j N_j} dV' \int \frac{dk k^4}{(k^2 + m^2)^{1/2}} \exp\left[-\frac{(k^2 + m^2)^{1/2}}{T}\right]$$

$$= V\left(1 - \sum n_j V_j\right) \lambda_i I_i \tag{22}$$

where λ_i is the fugacity of i-th species, I_i is the remaining part of the integral. Thus we can write the following equation of n_i :

$$n_i = (1 - R)\lambda_i I_i - I_i \lambda_i^2 \frac{\partial R}{\partial \lambda_i} \tag{23}$$

where $R = \sum n_j V_j$ is the fraction of the occupied volume. After simple manipulation, we get

$$R = (1 - R)\sum I_i \lambda_i V_i - \sum I_i \lambda_i^2 V_i \frac{\partial R}{\partial \lambda_i}. \tag{24}$$

We can solve the differential eq. (24) by using the method of parametric line and get

$$R = 1 - \left[\int_t^{\infty} e^{-t'/G(t')}\, dt' \Big/ \left(e^{-t/G(t)}\right)\right], \tag{25}$$

where $t = -1/I_1 V_1 \lambda_1$ and $G(t) = t(a_2 + I_2 V_2 t)(a_3 + I_3 V_3 t)\cdots$. Thus the values of some of the parameters are fixed arbitrarily. However, we can use the assumption that the number density of i-th species depends on its fugacity λ_i only and then $\partial R/\partial \lambda_i = \frac{\partial}{\partial \lambda_i}\left(\sum n_j V_j\right) = \frac{\partial n_i}{\partial \lambda_i} V_i$. Thus we get a simple differential equation as

$$\frac{\partial n_i}{\partial \lambda_i} + n_i\left[\left(1/I_i V_i \lambda_i^2\right) + \left(1/\lambda_i\right)\right] = \left(1 - \sum_{i \neq j} n_j V_j\right) / V_i \lambda_i. \tag{26}$$

Its solution can be written as

$$n_i = \frac{(1 - R)}{V}\left[Q_i / \left(\lambda_i \exp(-1/I_i V_i \lambda_i) - Q_i\right)\right], \tag{27}$$

where $$Q_i = \int_0^{\lambda_i} \exp\left(-1/I_i V_i \lambda_i\right) d\lambda_i,$$

$$R = \sum n_j V_j = X/(1 + X),$$

$$X = \sum Q_i / \left(\lambda_i \exp(-1/I_i V_i \lambda_i) - Q_i\right).$$

In Figures (8–9), we have shown the variations of baryonic pressure with temperature T and chemical potential μ_B, respectively for a multicomponent HG. We find that the prediction of our recent model lies close to the model of Rischke *et al* [11] and differs considerably from the inconsistent Kuono-Takagi model at large T and/or μ_B. In Figure 10 we have demonstrated the prediction of our model for the variation of the entropy per baryon S/B ratio with baryon chemical potential μ_B and we find maximum value of S/B in the present model. This means that the present experimental value of S/B around sixty can only be obtained in our present model which is thermodynamically consistent one.

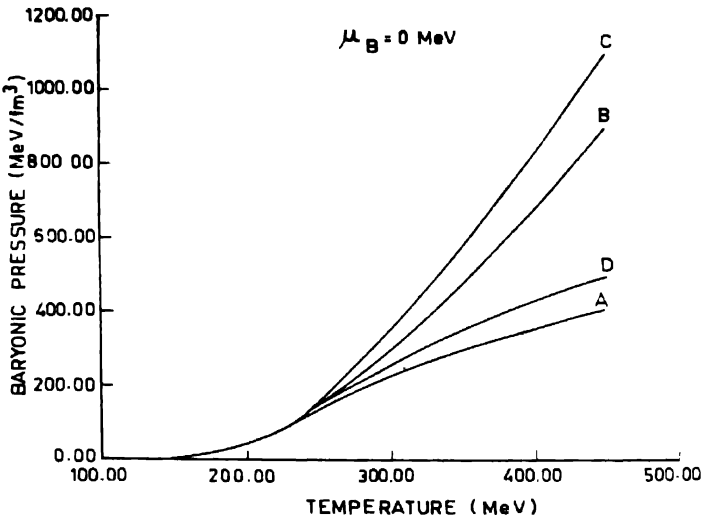

Figure 8. Baryonic pressure vs baryon chemical potential μ_B at T = 200 MeV in a multicomponent HG with N, Λ, Δ, Σ, Σ^*, Λ^*, Ξ baryonic components and K, K^* mesons for strangeness conservation. Curve A gives the prediction of the inconsistent approach of Kuono and Takagi. B yields the results of our present calculation and C that of Rischeke *et al*. D represents the curve obtained in the Uddin-Singh model.

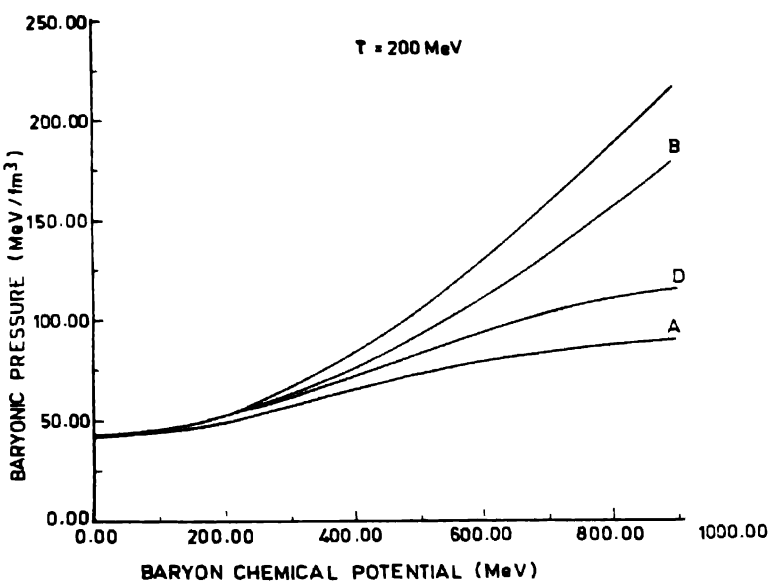

Figure 9. Variation of baryonic pressure with temperature at μ_B = 0 MeV. The notations for A, B, C, D are given in Figure 8.

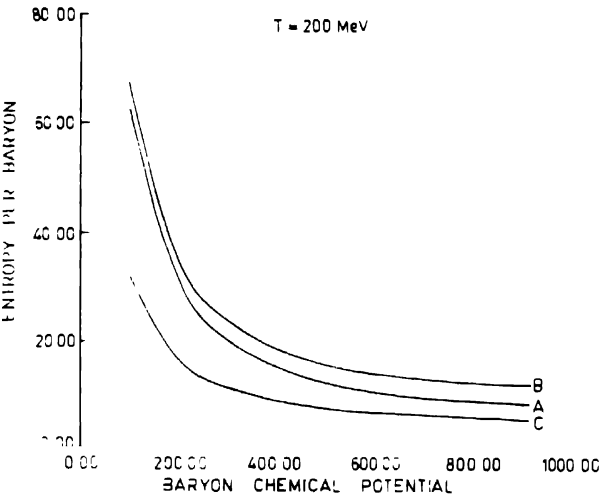

Figure 10. Variation of the entropy per baryon ratio S/B with baryon chemical potential μ_B at T = 200 MeV in the inconsistent model of Kuono and Takagi (curve A), our present thermodynamically consistent model (curve B) and the model of Rischke *et al* [11] (curve C)

5. QGP signals

The standard method for testing the QGP signals is to compare the predictions of nucleus-nucleus collision models incorporating the presence of a QGP with the prediction of models based entirely on the dynamics of colour-singlet hadrons. Unfortunately we do not have a proper theoretical understanding of high energy nuclear collisions [1]. The quantitative understanding of the background processes in the hadron gas is essentially a prerequisite The models of the HG vary from the thermal models where HG is considered as equilibrated statistical system to transport or cascade models which do not involve equilibrium concepts but are based on the superposition of hadron-hadron collisions. No one has yet devised a clean and unambiguous signal of QGP formation. Moreover, it is amazing to see that the existing data are explained both in thermal HG picture as well as in cascade model approach.

Strangeness abundance has been suggested to be one such signal. The idea is simple. In a baryon-dense hadron gas, we have

$$n_s = 6\int \frac{d^3p}{(2\pi)^3}\left[\left(\exp\left(p^2+m_s^2\right)^{1/2}/T\right)+1\right]^{-1}$$

$$n_{\bar{u}} = 6\int \frac{d^3p}{(2\pi)^3}\left[\left(\exp(p+\mu_q)/T\right)+1\right] \tag{28}$$

When $\mu_q > 200$ MeV and $m_s = 150$ MeV, $n_s > n_{\bar{u}}$. Similar results one obtains for $q\bar{q}$ symmetric (*i.e.* $\mu_q = 0$) system as well when $T \gg m_s$. Moreover, it is easier to produce s-

quark in QGP than K-meson in HG because $m_K > m_s$ and degeneracy factor for s quark is larger than that of K meson. Larger $n_{\bar{s}}/n_{\bar{u}}$ ratio in QGP means a larger K^+/π^+ ratio after hadronization of the QGP. Recent CERN experiments using sulphur-nucleus reactions have reported a strangeness abundance 3–5 times larger than observed in pp reactions. However, this rise in the strange particle production can be explained either by using thermal models or by hadron cascade models. Moreover, the rise in K^+/π^+ production can also be explained by considering a medium modification of hadronic parameters *e.g.* masses *etc.*

Asher Shor [15] inferred from large s and $\bar{s}$ quark densities that there would be an abundant production of ϕ mesons. Since ϕ production from ordinary hadronic processes, *e.g.* $\pi p \rightarrow \phi n$ and $pp \rightarrow \phi pp$ *etc.* are suppressed due to Okubo-Zweig-Iizuka (OZI) rule, so ϕ mesons from a hadron gas without QGP formation would be far too smaller in magnitude. The OZI rule forbids processes if they involve disconnected "hairpin" type quark-line diagrams. However, OZI rule is not exact and we invoke unitarity diagrams to explain such breaking. In the dual topological unitarization (DTU) scheme, the twists in the quark lines involved in the s-channel unitarity diagrams give rise to a cancellation mechanism and thus the suppression of amplitude is explained. However, the twists in the t-channel quark lines do not give rise to such cancellation mechanism. In other words, ϕ production in the fragmentation region (large μ-regime) is more suppressed than in the central region (small μ region). Thus we suggested that the variation of the ratio ϕ/ω with the baryon chemical potential can serve as a signature because this ratio rapidly decreases for a HG without any QGP formation whereas in the presence of a QGP matter, it is almost a constant [16]. However, we cannot infer about μ and T in a nucleus-nucleus collision unless we use an EOS for the matter. Recently we have suggested [17] that we can study the variation of $\phi/(\rho + \omega)$ either with baryon density n_B or energy density ε and this will give a potential probe for a QGP formation. In our calculation, we have used hadronic EOS proposed earlier and get the energy density $\varepsilon = TS + \mu n_i - P$. We take π, K, η, ρ, ω, η', K^*, ϕ, p, n, Λ, Σ, Ξ, Δ, Σ^* and Λ^* (1405 MeV) in our calculation for the quantities of HG.

For the calculation of the ratio $\phi/(\rho + \omega)$ from a QGP, we consider production of quarks and anti-quarks in the plasma during the equilibration of gluons in the mid-rapidity region and the probability for the emission of a particle with q quarks per unit of phase space volume is

$$P = \prod f_q \lambda_q g_q \gamma_q \exp\left(-E_q/T\right),$$

where f_q is the probability for creation of quarks by gluon fragmentation, m_q is the mass of the quark q, λq is the chemical fugacity, g_q is the degeneracy factor, γ_q is the relative equilibration factor and E_q is the energy of the quark. Thus after some assumptions, we get

$$\frac{\phi}{(\rho+\omega)} = \exp\left(-\frac{2\pi}{k} m_s^2\right).$$

We have used the same E_T window for the particles. In Figures. (11–12), we have shown the variation of the ratio with respect to ε and n_B respectively. We find for QGP formation,

$\phi/(\rho + \omega)$ remains constant around 0.4. However, for a HG without QGP, this ratio increases with ε and reaches a constant around 0.25. The variation of the ratio with n_B also

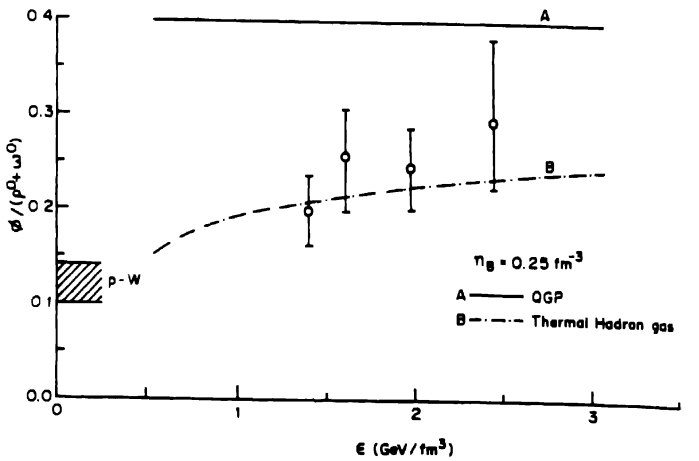

Figure 11. Variation of the ratio $\phi/(\rho^0 + \omega^0)$ with the baryon number density at a fixed energy density ε = 1 GeV/fm^3. The solid line represents the QGP contribution, the dash-dotted line indicates thermal hadron gas calculation and dashed line represents the contribution from the superposed hadron-hadron model

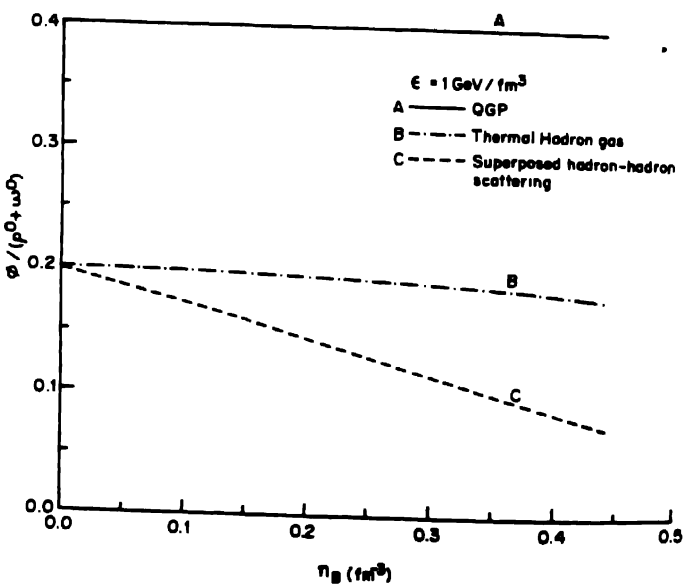

Figure 12. Variation of the ratio $\phi/(\rho^0 + \omega^0)$ with the energy density ε at a constant n_B = 0.25 fm^{-3}, solid line represents the QGP contribution and dash-dotted line represents the thermal hadron gas calculation. Experimental data are taken from [26].

shows a similar behaviour. Moreover, we find that variation of $\phi/(\rho + \omega)$ with n_B can also distinguish between a thermal picture and cascade picture of HG. Similar conclusions can be derived for other strange particles [18].

One important signature [19] for the QGP formation has been suggested as photons and dileptons production. Since these particles are subjected to electromagnetic interactions only, their mean free paths are larger and they are unaffected by the hadronization of the system. Since they reveal the thermal status of the fireball, these particles are known as thermometers. For dileptons from QGP, we have mainly the process $q\bar{q} \rightarrow \mu^+\mu^-$ whereas from a HG $\pi^+\pi^- \rightarrow \mu^+\mu^-$, $p\bar{p} \rightarrow \mu^+\mu^-$, $D \rightarrow \mu^+\mu^-$ as well as Drell Yan processes $pp \rightarrow \mu^+\mu^- X$ can contribute. Our main motivation is to identify some particle ratios or particle spectra which are much different from the HG background. Similarly for the photon production, $q\bar{q} \rightarrow g\gamma$, $qg \rightarrow q\gamma$, $\bar{q}g \rightarrow \bar{q}\gamma$ contribute in the QGP whereas $\pi\pi \rightarrow \rho\gamma$, $\pi\rho \rightarrow \pi\gamma$, $\rho \rightarrow \pi\pi\gamma$, $\omega \rightarrow \pi\gamma$ etc. contribute in the HG case. The situation as standing at present tells that HG contributions almost match with the QGP contributions.

One significant signature for QGP formation was the suppression in J/Ψ production as suggested by Matsui and Satz. The idea is that J/Ψ is mainly produced in the pre-equilibrium collision state. Since it has a large mass, its production from a thermally equilibrated system is not significant unless we have a very large temperature. J/Ψ then passes through a deconfining medium in the case of a QGP formation. So the resonance melts into $c\bar{c}$ quarks and they are separated by a large distance depending on the size of the

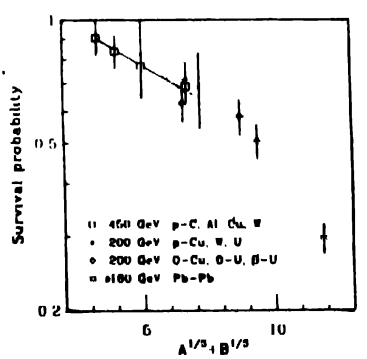

Figure 13. The J/Ψ survival probability after absorption through nuclear matter, as a function of $A^{1/3} + B^{1/3}$, where A and B are the mass numbers of the colliding objects. The full line (dotted line) is the survival probability for the proton-nucleus (nucleus-nucleus) systems, calculated with a cross section $\sigma_a = 6.2$ mb.

deconfining medium. Thus the possibility for a recombination into J/Ψ is very small. In comparison, for a HG without QGP formation only some of J/Ψ will be lost due to rescattering. So a suppression in J/Ψ production will signal a QGP formation. NA38 experiments with O–U at 200 GeV/A clearly show such suppression for J/Ψ peak in the

mass distribution of dileptons around 3.1 GeV. Moreover, J/Ψ suppression occurs more at lower p_T as expected for QGP formation. However, conventional explanations with nuclear absorption or rescattering can also explain J/Ψ suppression.

Recently, NA50 collaboration has reported [20] a strong suppression of J/ψ production in Pb–Pb central collisions at 158 GeV/A. The suppression is much stronger than the expected one from conventional explanations [21] which explain the previous data for O–U or S–U central collisions, as well as for the hadron-nucleus collisions. Thus NA50 data as shown in Figure 13, show a clear deviation from the previous situation [22]. It is believed that this new observation has given us the first clear hint for the deconfinement occurring in the ultra-relativistic heavy ion collisions.

6. Early universe scenario

In the early universe, the coloured quarks and gluons were deconfined and the matter existed in the form of QGP. As the universe expanded, the temperature dropped through the critical temperature T_c for the phase transition where the QGP could exist in thermal, mechanical and chemical equilibrium with a dense, hot HG. This could induce a large isothermal baryon number fluctuation which would change the standard scenario for primordial nucleosynthesis. The ratio of baryon number densities in the two phases is represented by a baryon contrast ratio $R = n_B^{QGP} / n_B^{HG}$ evaluated at $T = T_c$ and the baryon chemical potential $\mu_B = 10^{-10} T_c$. If $R \gg 1$, we get a thermodynamically favourable condition for the baryon number to reside predominantly in the QGP phase. Recently, several attempts have been made to determine the values of R using various types of equation of state (EOS) for the QGP as well as HG phases. These studies amply make it clear that the quark-hadron phase transition induces a large fluctuation in the baryon density in the early universe [23–25].

Acknowledgment

The author is grateful to the Department of Science and Technology (DST), New Delhi for a research grant.

References

[1] C P Singh *Phys. Rep.* **236** 147 (1993)
[2] C P Singh *Int. J. Mod. Phys.* **A7** 7145 (1992)
[3] B Muller *Rep. Prog. Phys.* **58** 611 (1995)
[4] S A Bonometto and O Pantano *Phys. Rep.* **228** 175 (1993)
[5] H Meyer-Ortmanns *Rev. Mod. Phys.* **68** 473 (1996)
[6] A Leonidov, K Redlich, H Satz, E Suhonen and G Weber *Phys. Rev.* **D50** 4657 (1994)
[7] B K Patra and C P Singh *Phys. Rev.* **D54** 3551 (1996)
[8] B K Patra and C P Singh *Z. Phys.* **C74** 699 (1997)
[9] R Hagedorn *Z. Phys.* **C42** 265 (1983)

[10] J Cleimans and E Suhonen *Z. Phys* **C37** 51 (1987)

[11] D H Rischke, M I Gorenstein, H Stöcker and W Greiner *Z Phys* **C51** 485 (1991)

[12] S Uddin and C P Singh *Z Phys* **C63** 147 (1994)

[13] C P Singh, B K Patra and K K Singh *Phys Lett* **B387** 680 (1996)

[14] J I Kapusta, A P Vischer and R Venugopalan *Phys Rev.* **C51** 901 (1995)

[15] A Shor *Phys. Rev Lett* **54** 1122 (1985)

[16] C P Singh *Phys. Rev. Lett* **56** 1750 (1986), *Phys Lett* **B188** 369 (1987)

[17] C P Singh, V K Tiwari and K K Singh *Phys Lett* **B393** 188 (1997)

[18] V K Tiwari, S K Singh, S Uddin and C P Singh *Phys. Rev* **C53** 2388 (1996)

[19] Jan-e Alam, Sibaji Raha and Bikash Sinha *Phys Rep* **273** 243 and references therein (1996)

[20] NA50 collaboration, M Govin *et al in Proceedings of Quark Matter* '96 edited by P Braun Munzinger *et al Nucl Phys* **A** (to be published)

[21] J P Blaizot and J Y Ollitrault *Phys Rev Lett* **77** 1703 (1996)

[22] N Armesto, M A Braun, E G Ferreiro and C Pajares *Phys Rev Lett* **77** 3736 (1996)

[23] C P Singh, B K Patra and S Uddin *Phys Rev* **D49** 4023 (1994)

[24] B K Patra, K K Singh, S Uddin and C P Singh *Phys Rev* **D53** 993 (1996)

[25] B K Patra and C P Singh *Nucl Phys.* **A614** 337 (1997)

[26] J Stachel and G R Young *Ann Rev Nucl Part Science* **42** 537 (1992)